Ecological Modelling 279 (2014) 89–99

Contents lists available at ScienceDirect

Ecological Modelling

journal homepage: www.elsevier.com/locate/ecolmodel

Spatial and temporal heterogeneity in the dynamics of eastern U.S. forests: Implications for developing broad-scale forest dynamics models

Tao Zhang[a,*], Jeremy W. Lichstein[a], Richard A. Birdsey[b]

[a] Department of Biology, University of Florida, P.O. Box 118525, Gainesville, FL 32611, USA
[b] Northern Research Station, USDA Forest Service, 11 Campus Boulevard Suite 200, Newtown Square, PA 19073, USA

ARTICLE INFO

Article history:
Received 19 June 2013
Received in revised form 14 February 2014
Accepted 15 February 2014
Available online 14 March 2014

ABSTRACT

Spatial and temporal environmental heterogeneity is known to play an important role in the dynamics of populations and communities. However, the implications of this heterogeneity for developing and testing regional- to global-scale forest dynamics models are largely unexplored. Predictions from forest dynamics models are typically compared to chronosequences assembled from forest inventory data using the space-for-time substitution approach, which assumes that different-aged stands across space have followed (and will follow) the same dynamics. Often, this assumption is invalid in the presence of spatial and/or temporal heterogeneity. We used the perfect plasticity approximation (PPA) forest dynamics model, parameterized with forest inventory data for >10 forest types in the eastern U.S., to diagnose spatial and temporal heterogeneity in forest dynamics, and to explore how this heterogeneity can affect comparisons between predicted dynamics and chronosequence observations. Our results provided evidence that spatial and temporal heterogeneity are widespread in eastern U.S. forests. Temporal heterogeneity was apparent because species whose observed abundances have increased over recent decades tended to be the same species for which predicted abundance (derived from individual-level growth and mortality rates estimated from the recent decades of inventory data) were greater than observed abundance. Spatial heterogeneity was apparent because species had more competitive parameter estimates (higher growth and/or lower mortality) on inventory plots where they are most abundant, relative to other plots in the same forest type. Spatial and temporal heterogeneity both contributed to mismatches between predicted dynamics and chronosequence observations. Predictions of canopy structure (proportion of individuals in the upper canopy vs. the understory) were well-matched to inventory data, suggesting that the PPA's simple space-filling algorithm was not an important source of error in predicting forest dynamics.

1. Introduction

Spatial and temporal environmental heterogeneity plays an important role in community and ecosystem dynamics (Kobe, 1996; Chesson, 2000; Clark et al., 2010). However, the implications of this heterogeneity for developing and testing regional- to global-scale models of ecological dynamics are largely unexplored. There is a growing interest in using geographically extensive forest inventory data sets, such as the U.S. Forest Service Forest Inventory and Analysis (FIA) database (http://www.fia.fs.fed.us/), to parameterize and test forest dynamics models (e.g., Purves et al., 2008; Caspersen et al., 2011; Vanderwel et al., 2013). Due to the limited availability of long-term data sets (i.e., continuous measurements of the same sample plots over multiple decades), model predictions of forest dynamics are typically compared to chronosequences assembled from inventory data using the "space-for-time substitution" approach (Pickett, 1989; Lichstein et al., 2009; Walker et al., 2010). This approach assumes that dynamics that occur over time in a given location can be inferred from different-aged stands sampled across space over a short time period. Clearly, this assumption is problematic if forest dynamics are heterogeneous over the temporal/spatial dimensions of the chronosequence data, as would be expected due to temporal changes in climate, forest management, and natural disturbance regimes, as well as unmeasured edaphic variation across the sampled stands.

* Corresponding author. Tel.: +1 352 273 0130; fax: +1 352 392 3704.
E-mail addresses: tz@ufl.edu, tz05@my.fsu.edu (T. Zhang), jlichstein@ufl.edu (J.W. Lichstein), rbirdsey@fs.fed.us (R.A. Birdsey).

http://dx.doi.org/10.1016/j.ecolmodel.2014.02.011
0304-3800/

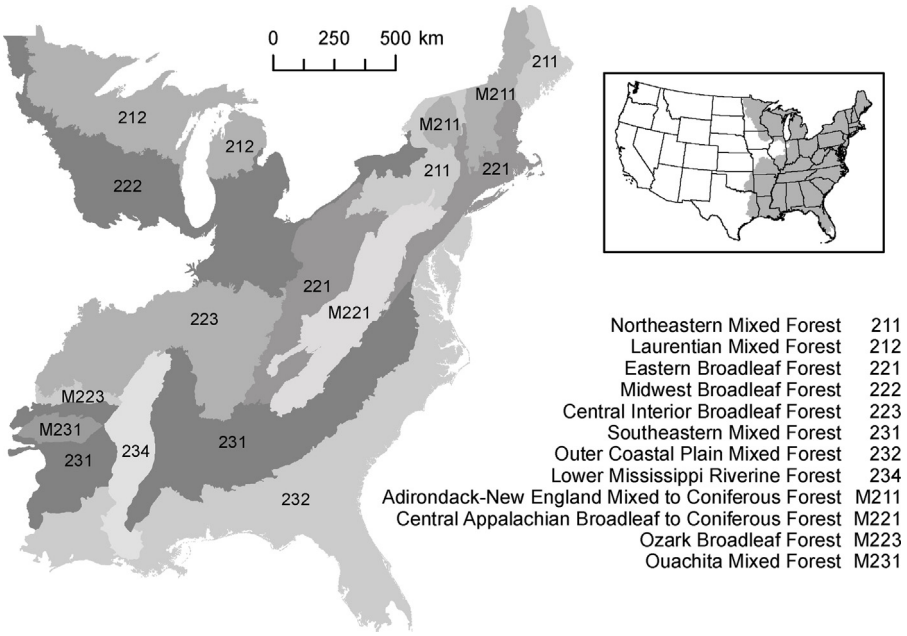

Fig. 1. Map of ecoprovinces reported in the U.S. Forest Inventory and Analysis (FIA) database (McNab et al., 2007; http://www.fs.fed.us/rm/ecoregions/products/map-ecoregions-united-states/). Ecoprovince codes beginning with an "M" denote mountain provinces. The forest types considered in this paper are defined by partitioning FIA plots within each ecoprovince shown in the figure into three broad soil types reported by FIA: xeric, mesic, and hydric.

The perfect plasticity approximation (PPA) forest dynamics model (Adams et al., 2007; Purves et al., 2007, 2008; Strigul et al., 2008; Dybzinski et al., 2011; Lichstein and Pacala, 2011; Bohlman and Pacala, 2012; Farrior et al., 2013) has been proposed as a candidate forest module for "next-generation" dynamic global vegetation models (DGVMs; Scheiter et al., 2013) that include individual-tree-level processes (e.g., Friend et al., 1997; Moorcroft et al., 2001; Sato et al., 2007). The PPA model holds promise for global-scale applications because it is mathematically and computationally tractable, captures the essence of height-structured competition among individual trees, and can be parameterized from widely available forest inventory data. Purves et al. (2008) parameterized the PPA model for four soil types in the north-central U.S. using individual-level growth and mortality rates and allometry observed over recent decades. Purves et al. (2008) then compared dynamics of secondary succession predicted by the PPA model to those inferred from forest chronosequences. Although predicted biomass dynamics were similar to the chronosequences at the stand level (i.e., all species combined), there were large discrepancies between predicted dynamics and observed chronosequences at the individual species level on some soil types. Purves et al. (2008) suggested that these mismatches may reflect, in part, temporal and/or spatial heterogeneity in forest dynamics that violate the "space-for-time substitution" assumptions (Pickett, 1989; Lichstein et al., 2009; Walker et al., 2010). Purves et al. (2008) provided some anecdotal evidence in support of this argument, but reported no quantitative tests.

In this study, we used geographically extensive forest inventory data to parameterize the PPA model for different forest types in the eastern U.S. (Fig. 1) and to test model predictions of canopy structure and forest dynamics. We were particularly interested in evaluating the effects of spatial and temporal heterogeneity on mismatches between PPA-predicted forest dynamics and chronosequences assembled from FIA data (hereafter referred to as "model-data mismatches"). Numerous previous studies have documented shifts in forest dynamics over time or across spatial edaphic gradients (e.g., Kobe, 1996; van Breemen et al., 1997; Allen and Breshears, 1998; Orwig et al., 2001; Kardol et al., 2010). However, to our knowledge, the implications of these forms of heterogeneity for developing and testing broad-scale forest dynamics models from geographically extensive inventory data have not previously been explored. Before describing our methods, we briefly introduce the PPA model, and we explain in more detail how temporal and spatial heterogeneity may affect model-data comparisons.

1.1. The PPA forest model

Strigul et al. (2008) provide a detailed description of the PPA model. The key elements of the "flat-top" version of the model used here (in which we assume that tree crowns have flat tops) are summarized in Appendix A-1 and in Lichstein and Pacala (2011). The defining characteristic of the PPA model is the assumption that individual trees are infinitely plastic in arranging crown area in horizontal space so as to minimize vertical overlap (shading among individuals). According to this assumption, the upper canopy is filled by the tallest set of trees whose collective crown area is equal to the ground area (e.g., the size of a stand or plot in horizontal space). The height of the shortest tree in this upper layer is labeled Z^*, and subsequent layers may be similarly defined (Bohlman and Pacala, 2012). Light availability is assumed to be uniform within each layer and to decrease from taller to shorter layers. Furthermore, in this paper (as in Purves et al., 2008), we assume that the amount of shade cast by a given layer is independent of the size or species identity of the trees in the layer. The PPA representation of vertical forest structure leads to a simple demographic model of forest dynamics (see Section 2).

1.2. Temporal heterogeneity

Changes in climate, disturbance regimes, and other factors may cause shifts over time in the relative competitive abilities, and therefore abundances, of different species. In a forest dynamics model, a species' competitive ability reflects its performance during the time period that the data used to parameterize the model were collected. Thus, if the model is parameterized from growth and mortality rates of different species in inventory plots measured over a single recent decade (e.g., 2000–2010), the most competitive species during this decade (e.g., the species with the highest

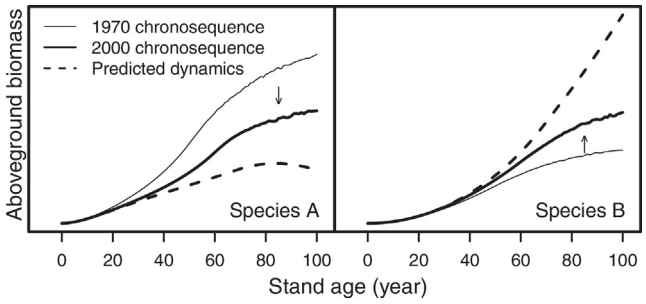

Fig. 2. Illustration of how temporal heterogeneity may cause mismatches between predicted and observed abundance for two competing species. The figure assumes that between the years 1900 and 2000, the mortality rates of species-A individuals gradually doubled (decreasing competitive ability), whereas the mortality rates of species-B individuals gradually deceased by 50% (increasing competitive ability). These changes in competitive ability cause shifts in abundance over time, as seen in the difference between chronosequences constructed using the space-for-time substitution in 1970 and again in 2000. The dashed curve shows the dynamics predicted by the PPA model described in Section 2, using the average mortality rates of the species from 1990 to 2000. Thus, the figure illustrates how trends in species competitive ability can cause mismatches between predicted dynamics (which are determined by species competitive abilities at the time the model is parameterized) and observed chronosequences (which reflect species competitive abilities integrated over the entire age of the chronosequence). The mismatches between predicted and chronosequence abundance are in the same direction as the temporal trend in chronosequence abundance, as shown by the arrows.

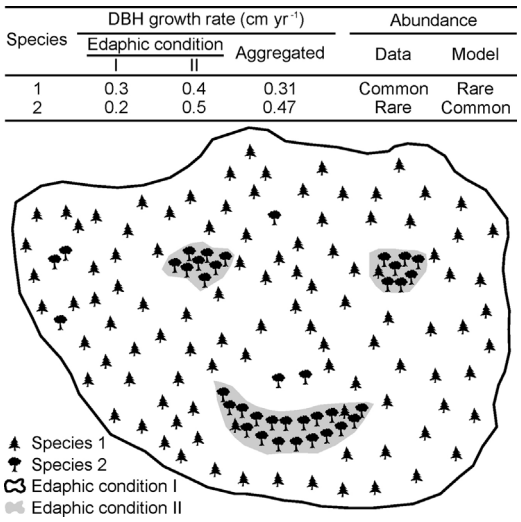

Species	DBH growth rate (cm yr^{-1})			Abundance	
	Edaphic condition		Aggregated	Data	Model
	I	II			
1	0.3	0.4	0.31	Common	Rare
2	0.2	0.5	0.47	Rare	Common

Fig. 3. Illustration of how spatial heterogeneity may cause mismatches between predicted and observed abundance for two competing species within a single forest type. The illustrated example assumes that there are two "hidden" (unrecognized) edaphic conditions (I and II) that are aggregated when estimating species-level model parameters within the forest type. Species 1 is the competitive dominant in the common condition I, and species 2 is the competitive dominant in the relatively rare condition II (which is also the more productive condition), as indicated in the table of diameter growth rates. Although species 2 (being mostly restricted to the rare condition II) is in reality rare, its parameter estimates in the aggregated data set (see table) are more competitive than species 1's, which results in high model-predicted abundance of species 2. The aggregated diameter growth rates in the table assume that 90% of species 1 individuals occur in condition I, and 90% of species 2 individuals occur in condition II. For simplification, this illustration does not consider how growth and mortality rates vary across canopy layers. In the PPA model, growth and mortality rates of a species are different across canopy layers, as described in Section 2.

growth rates and/or lowest mortality rates) would be predicted by the model to be the most abundant species. However, species abundances in an inventory plot reflect the cumulative result of competition over the entire age of the plot. The most competitive species in a recent decade was not necessarily the most competitive species over the history of stand development. Species whose competitive ability relative to co-occurring species has increased (decreased) over recent decades should tend to have increasing (decreasing) relative abundance over this same period. Therefore, temporal heterogeneity should result in a positive correlation between species' model-data mismatches and species' temporal trends in abundance as measured from inventory data. A simple illustration of the temporal heterogeneity effect on model-data mismatches is presented in Fig. 2.

1.3. Spatial heterogeneity

Within a given forest type, which we define as a unique combination of the ecoprovinces (Fig. 1) and broad soil types (xeric, mesic, or hydric) reported by FIA for each inventory plot, different species may hold a competitive advantage in different stands due to specialization on edaphic, climatic, or other environmental variables that vary spatially within forest types. In this case, aggregating forest inventory data over spatially variable conditions may introduce parameter estimation errors that lead to mismatches between predicted and observed forest dynamics. Fig. 3 provides a simple illustration of how spatial heterogeneity may affect model-data comparisons. In this hypothetical case, two species compete with each other, and each is more competitive in one of two edaphic conditions within a soil type. As Fig. 3 illustrates, parameters estimated from the aggregated data could lead to reversals in the rank order of species abundances between the model and reality.

2. Methods

We first briefly describe the publicly available U.S. Forest Inventory and Analysis (FIA) database (http://www.fia.fs.fed.us/), the primary data source for our analyses. The online FIA database includes a systematic sample of all U.S. forests, on both public and private land, dating to as early as ~1970 in some U.S. states. FIA subdivides the U.S. land area into 2400-ha hexagons, and one randomly located inventory plot is sampled within each hexagon if the location fulfills FIA criteria for being considered "forest" (Reams et al., 2005). The sampling design was standardized across the U.S. around 1999. In the standardized design, plots consist of four subplots distributed over a 0.4 ha area. Subplots are 7.3 m radius and all trees with a diameter at breast height (DBH) $\geq$ 12.7 cm in the subplots are measured. Within each subplot, saplings (trees with DBH > 2.5 and < 12.7 cm) are measured in one 2.1 m-radius microplot (Bechtold and Scott, 2005). Similar data were collected at a national scale prior to 1999, but the exact plot design varied across U.S. states. Although the area actually measured in each inventory plot is only 0.067 ha, the large number of locations (~100,000) includes data on millions of individual trees.

2.1. Evaluating PPA canopy layer predictions

To evaluate the capacity of the PPA model to reproduce observed patterns in canopy structure, we compared the proportion of individuals in FIA plots predicted by the PPA model to be in the upper canopy ($PCAN_{PPA}$; as opposed to the understory) to the corresponding observed proportion calculated from FIA data ($PCAN_{FIA}$). We calculated $PCAN_{PPA}$ and $PCAN_{FIA}$ for each species in each forest type with at least 30 individuals in the FIA data set. To calculate $PCAN_{FIA}$, we used crown classes reported by FIA for individual trees: open-grown, dominant, co-dominant, intermediate, or overtopped (Woudenberg et al., 2010). We excluded FIA plots with any open-grown trees because such trees indicate non-forest conditions. We calculated $PCAN_{FIA}$ using two different assumptions: (1) we considered only dominant and co-dominant trees to be in the upper canopy, and (2) we considered dominant, co-dominant, and intermediate trees to be in the upper canopy. These two

methods provide reasonable lower and upper bounds for $PCAN_{FIA}$. To calculate $PCAN_{PPA}$, we used allometries to estimate the crown area and tree height for each individual tree in each FIA plot (see Appendix A-2 for detail of allometric parameter estimation). We then used these estimated heights and crown areas to calculate the PPA model-predicted height of canopy closure (Z^*) for each FIA plot (see Appendix A-4 for Z^* calculation), which allowed us to generate a PPA model prediction for the canopy status of each individual: upper canopy (tree height $\geq Z^*$) or understory (tree height $< Z^*$).

The above PCAN predictions depend only on the DBH distributions reported in FIA plots (which are taken as given, rather than predicted, for the PCAN model-data comparison), the PPA Z^* criterion for assigning canopy layers, and the estimated height and crown-area allometries. Because the above PCAN predictions can affect, but are not affected by, the dynamical predictions of the PPA model (see Section 2.3), we can assess if PCAN errors are important sources of error in the dynamical predictions. If this were the case, then we would expect forest types with relatively large PCAN errors to also have relatively large errors in dynamical model predictions.

2.2. Parameter estimation

The PPA model requires parameters that describe growth, mortality, height allometry, crown-area allometry, and fecundity. Following Purves et al. (2008), we assumed a single fecundity value for all species (number of size-zero individuals produced per unit canopy area per year). We used the fecundity value 0.01 m^{-2} yr^{-1} for all species and forest types, which is similar to the values that Purves et al. (2008) estimated by tuning the PPA model to reproduce observed sapling densities in the north-central U.S. Our simplistic fecundity assumption likely introduces model errors, but is unlikely to systematically bias our evaluations of the impacts of temporal and spatial heterogeneity because simulated dynamics are less sensitive to fecundity than to growth and mortality rates (Purves et al., 2008, Appendix 2).

Growth, mortality, and height allometry parameters were fit to post-1999 FIA data (accessed from http://www.fia.fs.fed.us/ in November 2011). Crown-area allometry parameters were fit to data collected during the 1990s by the U.S. Forest Service Forest Health Monitoring (FHM) program (http://www.fia.fs.fed.us/tools-data/other_data/default.asp). Diameter growth rate (annual DBH increase; cm yr^{-1}) and annual mortality rate (yr^{-1}) are forest-type-, species-, and canopy-layer-specific parameters in our study. Growth and mortality differences across canopy layers account for some of the size-dependence typically observed in these rates (e.g., Pacala et al., 1994; Canham et al., 2004), but we ignored size-dependence in diameter-growth and mortality within each canopy layer. To assess the impact of this simplifying assumption, we performed experiments in which diameter growth rates of large trees declined according to the "constant area increment law" (Pacala et al., 1996) and mortality rates of large trees were assumed to double when the basal-area growth rate reaches its upper limit. These modifications reduced model-predicted biomass in old stands, but had little effect on species relative abundances (and thus had little effect on our species-level evaluations). We only report results based on the simpler size-independent assumptions. We assumed a forest-type- and species-specific height-DBH allometry of the form $H = h_1 DBH^{h_2}$, where H is tree height (m), h_1 and h_2 are parameters. Allowing for canopy-layer-specific height-allometry parameters did not significantly improve fits to data. Due to limited sample sizes in FHM data, we fit crown-area allometries at the species-level only, and we applied these to all forest types and all canopy layers. We assumed an allometry for individual crown area (m^2) of the form $CA = c_1 DBH^{c_2}$, where c_1 and c_2 are parameters (see Appendix A-2 for details).

We estimated growth, mortality, and height allometry parameters using maximum likelihood. Because selective logging can affect stand biomass dynamics and the growth and mortality rates of unharvested trees, we estimated model parameters and performed simulations based on two different data sets: Unfiltered and No-Harvest. For the Unfiltered case, parameter estimates for growth, mortality, and height allometry were based on all non-plantation (naturally regenerated) post-1999 FIA plots. For the No-Harvest case, we excluded FIA plots where any trees were reported to be affected by logging during the remeasurement interval (~5 years). For crown-area allometries, we adopted a taxonomically-structured hierarchical Bayesian modeling approach (Lichstein et al., 2010) due to the limited sample sizes in the FHM dataset. Methods for estimating parameters are described in detail in Appendix A-2. Forest dynamics simulations in each forest type included only those species whose maximum likelihood estimates of growth and mortality rates for both the upper-canopy and understory layers were robust (i.e., numerical convergence of maximum likelihood estimates and confidence intervals). Parameter estimates for these species, which included the most common species in each forest type, are reported in the tables in Appendix A (Tables S1–S4).

2.3. PPA simulations

In this study, the maximum number of species included in a simulation was 10. For each data set (Unfiltered and No-Harvest) in each forest type, we performed 100 simulations, each initialized with a nominal stand age of 15 years and continuing to an age of 120 years. The 100 replicate simulations propagated uncertainty in initial conditions (size distribution and species composition of a 15 year-old forest) and parameter estimates for growth, mortality, and allometry (see Appendix A-3 for details on simulation methods and error propagation). The initial condition in each of the 100 simulations combined information from randomly selected young FIA plots (see below), and each simulated community was assumed to be horizontally homogeneous (i.e., the PPA Z^* criterion was applied uniformly to the entire simulated community at each time step to assign individuals to different canopy layers; see Appendices A-1 and A-4 for more details). Thus, each simulation represents the dynamics of a single forest stand, starting from a young stand whose species composition reflects the population of trees across the entire forest type.

Following Purves et al. (2008), we used the PPA to simulate the dynamics of cohorts, which are defined by three properties: species identity, individual size (assumed equal for all individuals in a cohort), and spatial density (number of individuals per unit area). We initialized cohorts of a 15-year-old stand of a given forest type by (1) randomly selecting 50 plots with replacement from 10–20 year-old post-1999 FIA plots in a given forest type, (2) defining one initial cohort for each individual tree in these selected plots using the individual's species identity, DBH, and spatial density (ha^{-1} values reported by FIA divided by 50, the number of plots aggregated in our initial condition), and (3) applying a correction factor to the above spatial density to account for the fact that not all species that occurred in FIA plots were included in model simulations (see Appendix A-3 for details).

We simulated the dynamics from 15 to 120 years of age with an annual time step, starting with the initial cohorts described above. Within each time step, we (1) used the PPA Z^* criterion to assign each cohort to a canopy layer (we allowed for multiple understory layers following Bohlman and Pacala, 2012), (2) updated the DBH and density of each cohort according to its growth and mortality rates, respectively, and (3) added new size-zero cohorts to reflect reproduction. We considered several reproduction scenarios, all of which included as the main form of reproduction the product of the

fecundity rate (per-unit sun-exposed crown area) and the crown area of a given species in the top canopy layer (Purves et al., 2008). The alternative scenarios included different treatments of local vs. regional seed rain, but all yielded similar results (see Appendix A-3 for more details). We also considered plot-scale simulations in which the initial condition reflected a single FIA plot, rather than an aggregate of 50 randomly selected plots. We used the forest-type-level parameter estimates for these plot-scale simulations, because insufficient data were available to estimate parameters at the plot scale. Results of the plot-scale simulations are not reported, as they were qualitatively similar to the aggregate forest-type-level simulations.

We compared the PPA-predictions to FIA chronosequences of aboveground biomass (AGB; Mg C ha^{-1}) dynamics at both community and species levels (where "community" means AGB of all species combined). We estimated AGB of individuals from DBH in both the PPA predictions and FIA chronosequences using published biomass allometries (Jenkins et al., 2003) and assuming that C comprises 50% of biomass. We applied correction factors to species-level FIA chronosequences to account for species-level differences between the model and data caused by the exclusion of rare species from our simulations (see Appendix A-3 for details). We quantified community- and species-level model-data mismatches using the percent bias (PBIAS; Yapo et al., 1996):

$$PBIAS = \frac{\sum(PPA_t - FIA_t)}{\sum FIA_t} \times 100\% \quad (1)$$

where PPA_t is the mean PPA-simulated AGB value in a forest of age t, and FIA_t is the mean AGB value at age t in the FIA chronosequence. PBIAS values near zero indicate no systematic tendency for predictions to over- or underestimate FIA chronosequence values, whereas positive and negative values of PBIAS indicate over- and underestimation, respectively (Yapo et al., 1996).

2.4. Evaluating the impacts of heterogeneity on model-data mismatches

As described above, temporal heterogeneity should lead to a positive correlation between species-level model-data mismatches in AGB (quantified by PBIAS) and temporal trends in species abundance. For example, species with highly competitive PPA model parameter values (estimated from post-1999 inventory data) but low abundance in FIA chronosequences (which reflect ~100 years of forest dynamics) should have positive PBIAS, as well as increasing relative abundances over time. To test this hypothesis, for each forest type we calculated the relative abundance (proportion of total community biomass) of each species in the FIA data for the pre- and post-1999 time periods, and we quantified the temporal abundance trend as the ratio of post-1999 abundance to pre-1999 abundance. We restricted these calculations to 20–40 year-old plots in each time period, because 20 years should be long enough for differences in sapling growth and mortality rates (as opposed to earlier phases of recruitment, such as seed rain) to strongly affect patterns in sapling abundance, while 40 years should be young enough for abundances to be largely determined by recent individual performance (as opposed to historical factors operating over longer time scales).

To evaluate the effects of spatial heterogeneity on model-data comparisons, we hypothesized that if spatial environmental (e.g., edaphic) heterogeneity had a strong impact on forest dynamics, then PPA parameters for a given species should be more competitive if estimated only from FIA plots where the species is abundant, compared to parameter estimates obtained from all data aggregated across a given forest type. To test this hypothesis, we focused on PPA predictions for the most abundant species in each of two stand-age classes in each forest type: 40–60 and 80–100 years old. Age classes younger than 40 years do not allow for useful tests because predicted abundances in young stands are primarily determined by model initial conditions drawn from 10–20 year-old FIA plots. For each focal species in each forest type, we defined its high-abundance data set ($DATA_{HA}$) as the subset of FIA plots in its top 25th abundance percentile. We refer to the parameter estimates derived from $DATA_{HA}$ as θ_{HA}. Similarly, we refer to the complete set of FIA plots in each forest type and the associated parameter estimates as $DATA_{ALL}$ and θ_{ALL}, respectively. We tested two predictions for both 40–60 and 80–100 year-old age classes: the dominant (i.e., most abundant) FIA species should (1) be correctly predicted by θ_{HA} more often than by θ_{ALL}; and (2) have higher predicted abundance in simulations using θ_{HA} compared to θ_{ALL}. Within each pair of simulations (θ_{HA} vs. θ_{ALL}), the initial cohorts and the list of species included in the simulations were identical (i.e., we only included species for which θ_{HA} parameter estimates were available). We repeated these simulation experiments using three different types of initial conditions: 15-year-old $DATA_{ALL}$ stands, 15-year-old $DATA_{HA}$ stands, and zero-biomass stands. Initial cohorts for the two 15-year-old stand conditions were created the same way as described above (see Section 2.3). In the zero-biomass case, there was no initial cohort and colonization was solely from regional seed rain. For each type of initial condition, we performed 100 replicate simulations to propagate uncertainty in parameter values and (in the non-zero-biomass cases) initial conditions.

3. Results

3.1. Canopy layer predictions

The PPA accurately predicted PCAN. For the No-Harvest data, the overall $PCAN_{PPA}$ (all species and forest types pooled) was 45.4%, which was near the midpoint of the lower (35.7%; dominant and co-dominant crown classes) and upper (55.3%; dominant, co-dominant, and intermediate crown classes) estimates for $PCAN_{FIA}$. At the forest type level, 10 out of 12 forest types had a $PCAN_{PPA}$ that was within the bounds of $PCAN_{FIA}$. The errors, defined as the difference between $PCAN_{PPA}$ and the midpoint of the two $PCAN_{FIA}$ estimates, are only 4.7% on average and have no significant over- or under-estimation tendency (P-value = 0.76 for the null hypothesis that over- and under-estimations are equally likely). When species within forest types were examined, $PCAN_{PPA}$ was within the bounds of $PCAN_{FIA}$ in 63.2% out of 627 cases (Fig. 4). For the abundant species (113 cases), $PCAN_{PPA}$ was within the bounds of $PCAN_{FIA}$ 80.5% of the time (Fig. 4). The results for the Unfiltered data (Fig. S1) were similar to the No-Harvest results described above.

Errors in $PCAN_{PPA}$ were not correlated with the AGB mismatch index PBIAS (Eq. (1)) at either community or species levels. For the No-Harvest case, the community-level (across forest types; n = 12) rank correlation was 0.19 (P-value = 0.56), and species-level (within forest types; n = 8–10) rank correlations ranged from −0.52 to 0.52 (P-values ≥ 0.13). The species-level rank correlation across all forest types combined was −0.05 (P-value = 0.56; n = 113). Similarly, for the Unfiltered case, errors in $PCAN_{PPA}$ were not correlated with PBIAS at either community or species levels (detailed results not reported).

3.2. PPA predicted dynamics vs. FIA chronosequences of aboveground biomass

For the No-Harvest data, PPA predicted greater community AGB than observed in FIA chronosequences (Fig. 5a). PBIAS was positive in 12/12 cases and greater than 25% in 9/12 cases (Fig. 6). In contrast, for the Unfiltered data, PPA predictions of community AGB were similar to FIA chronosequences (Fig. 5b), with 11/16 forest

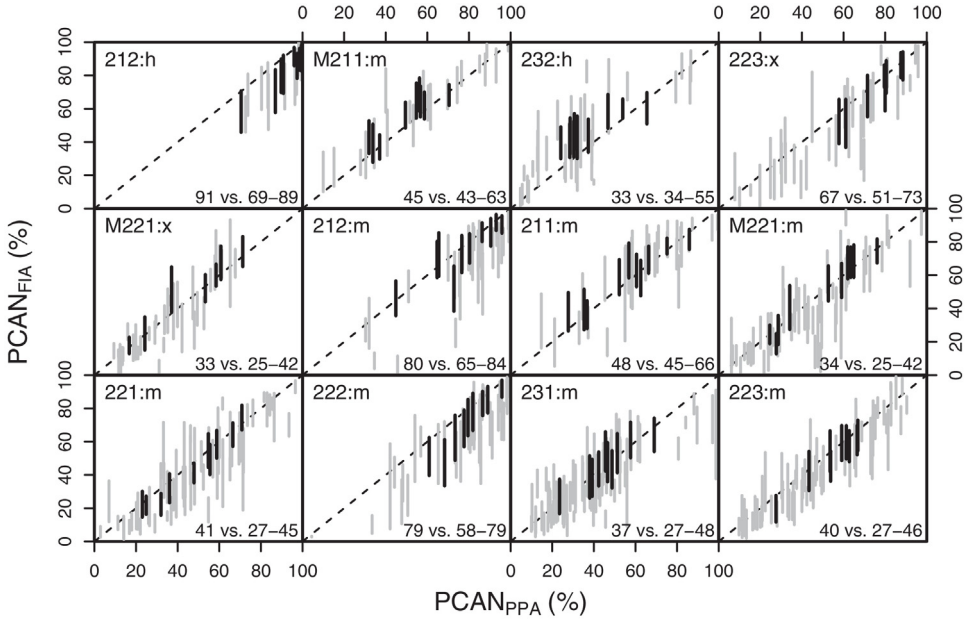

Fig. 4. Predicted vs. observed proportion of individuals in the upper canopy. Codes in the top left of each panel identify the forest type, defined by a combination of an FIA ecoprovince (Fig. 1) and soil type (x = xeric; m = mesic; h = hydric). In each forest type, the predicted proportion ($PCAN_{PPA}$) was calculated by applying the PPA Z^* criterion to individual FIA plots to predict the canopy status (upper canopy vs. understory) of individual trees. Upper bounds of the observed proportion ($PCAN_{FIA}$) were calculated by assigning the FIA crown classes dominant, co-dominant, and intermediate to the upper canopy. Lower bounds for $PCAN_{FIA}$ were calculated by assigning only the dominant and co-dominant crown classes to the upper canopy. Each vertical line segment represents a single species in a given forest type. Black symbols refer to common species (included in our simulations), and gray symbols refer to rare species (excluded from simulations). The forest-type-level proportions (all species pooled) are reported in the lower-right corner of each panel ($PCAN_{PPA}$ vs. $PCAN_{FIA}$ range). Results are for the No-Harvest data set. Results for the Unfiltered data are in Fig. S1.

types having |PBIAS| less than 25% (Fig. 6). For the well-matched forest types (|PBIAS| < 25%), PPA-predicted tree size distributions for mature forest (95 years old) were consistent with FIA data, whereas for most poorly-matched forest types, PPA size distributions showed elevated tree densities (relative to FIA data) in large DBH classes (Fig. 7 for No-Harvest data and Fig. S2 for Unfiltered data). "Humps" in large DBH classes in PPA size distributions reflect the simulation initial conditions, and indicate that the simulated 95 year-old forests in Fig. 7 and Fig. S2 are still far from the monotonically decreasing equilibrium size distribution (Strigul et al., 2008).

For both the No-Harvest data and the Unfiltered data, large mismatches in community AGB were often primarily due to one or two species with much higher AGB in PPA simulations compared to FIA chronosequences (e.g., Fig. 8c). In the nine No-Harvest cases with PBIAS > 25%, *Liriodendron tulipifera* had much greater predicted than observed AGB in seven cases; and *Pinus strobus* had higher predicted AGB in four cases. In the five Unfiltered cases with PBIAS > 25%, these two species were associated with large AGB mismatches in four and three cases, respectively. Among the forest types with a good community-level match between PPA and FIA, some also had good species-level matches (e.g., Fig. 8a), while others had poor species-level matches (e.g., Fig. 8b).

3.3. Impact of temporal heterogeneity on model-data mismatches

Species-level PBIAS and temporal trends in species relative abundance were positively correlated in most forest types, which supports the Temporal Heterogeneity Hypothesis. For the No-Harvest data, 11 out of the 12 forest types had positive rank correlations between PBIAS and the abundance trend (P-value = 0.003 for null hypothesis that positive and negative rank correlations are equally likely) (Fig. 9). With all forest types combined, the rank correlation between PBIAS and the abundance trend was 0.37 (P-value = 5.1×10^{-5}; n = 113). For the Unfiltered data, FIA records for the pre-1999 period were available for only 14 out of 16 forest types. Of these 14 forest types, 12 showed positive rank correlations between PBIAS and the abundance trend (P-value = 0.006 for null hypothesis that positive and negative rank correlations are equally likely) (Fig. 9). With all forest types combined, the rank correlation was 0.33 (P-value = 1.2×10^{-4}; n = 130).

3.4. Impact of spatial heterogeneity on model-data mismatches

The results also show that spatial heterogeneity contributes to the model-data mismatches: PPA model predictions for the observed dominant species were more accurate when model parameters in a given forest type were estimated from FIA plots where the dominant species was most abundant (parameters θ_{HA}) rather than from all plots (parameters θ_{ALL}). In terms of correctly predicting the identity of the FIA-observed dominant species, out of all the 12 cases examined (No-Harvest or Unfiltered × two age classes × three simulation initial conditions), θ_{HA} outperformed θ_{ALL} in 10 cases and performed equally well in the other two cases (Table 1). Predicted abundance for the FIA-observed dominant species was higher in simulations with θ_{HA} compared to θ_{ALL} in all 12 cases (Table 1).

4. Discussion

Our analyses indicate a good match between PPA model predictions of canopy structure and observations, but often poor matches between PPA model predictions of community (stand-level) biomass and species composition. As explained below, mismatches between predicted and observed stand-level biomass are at least partially due to overly simplistic assumptions of size-independent growth and mortality, which could easily be addressed in future versions of the PPA model. In contrast, species-level model-data mismatches are probably primarily due to spatial and temporal heterogeneity in species demographic rates, which are more difficult to address. Below, we discuss these results and their implications in details, and conclude by discussing alternative

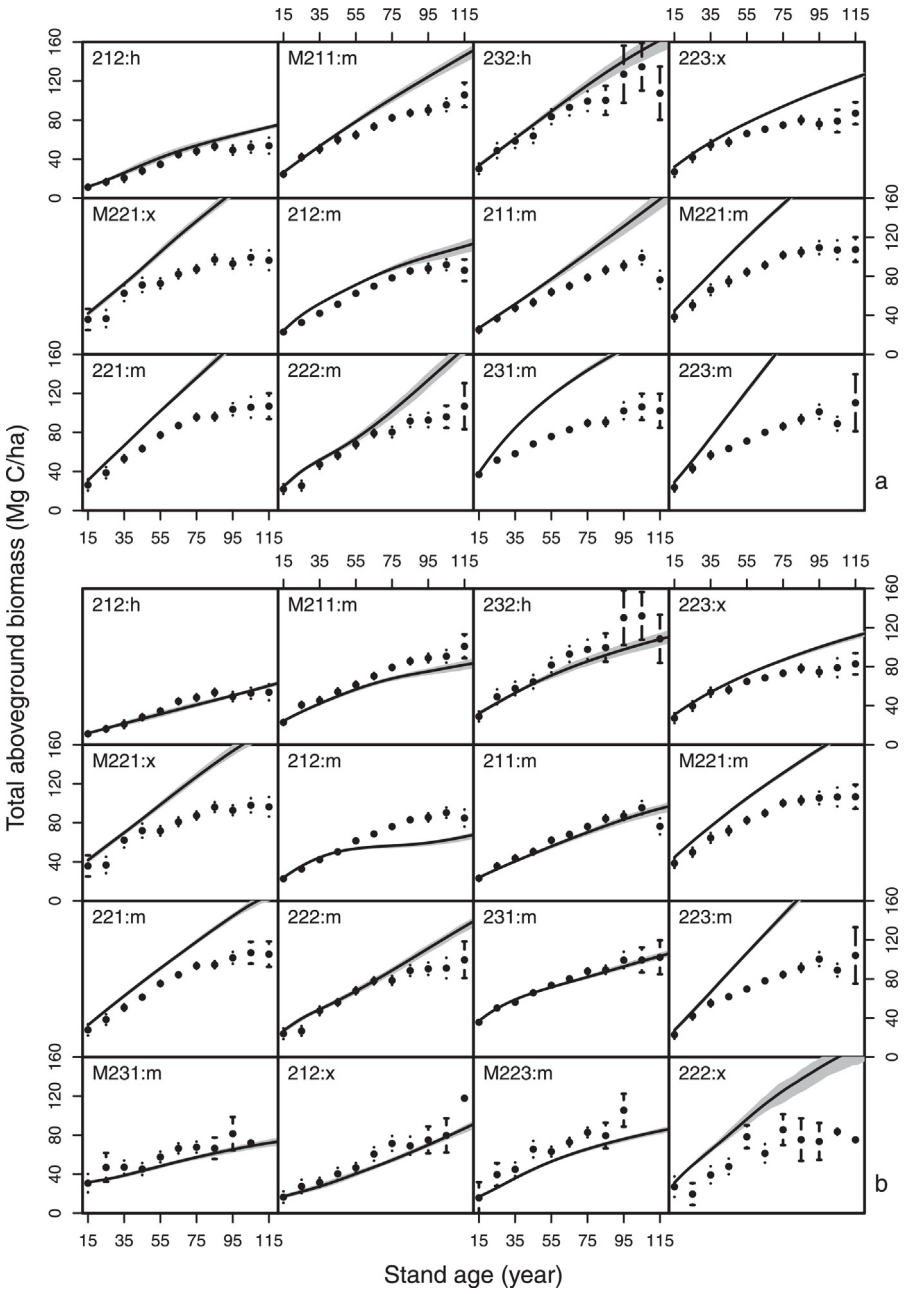

Fig. 5. Predicted (PPA; solid curves and shading) and observed (FIA data; points and error bars) community-level aboveground biomass dynamics for different forest types (codes in the top left of each panel). Panel (a) is for the No-Harvest case and (b) is for the Unfiltered case. Individual tree growth and mortality rates for PPA simulations were parameterized from post-1999 FIA plots (~5 year remeasurement interval), and simulations were initialized with data from 10–20 year-old FIA plots. To propagate uncertainty in initial conditions and parameter estimates, simulations were replicated 100 times for each forest type. Curves show the mean of these 100 simulations, and gray shading spans their 25th and 75th percentiles. Points and error bars show FIA means and their 95% confidence intervals in 10-year age classes. See Fig. 4 for explanation of forest type codes.

strategies to developing and testing broad-scale forest dynamics models.

4.1. Canopy layer predictions

The simple, flat-topped crown shapes assumed here and in most other applications of the PPA model yielded accurate predictions of the proportion of individuals in the upper canopy vs. the understory (PCAN; Fig. 4 and Fig. S1). The minor PCAN errors that did occur were not correlated with the degree of mismatch between predicted aboveground biomass (AGB) dynamics and observed AGB chronosequences. This suggests that model-data mismatches in AGB dynamics are due primarily to reasons other than the PPA space-filling algorithm (the "Z^* criterion") used to assign trees to different vertical canopy layers.

The PCAN calculations presented here were derived solely from the PPA Z^* criterion and allometries estimated from individual-level observations of crown area and tree height. Thus, the canopy structure tests presented here, like those presented in Bohlman and Pacala (2012), are completely independent of the test data. This is in contrast to the analysis of Purves et al. (2007), who used inverse modeling to fit crown shapes to PCAN observations. In most cases, our PCAN predictions were within the uncertainty range of the observations, despite the fact that we ignored intraspecific variation in height and crown-area allometries due to, for example, canopy-layer or soil-type effects. Preliminary analyses (not shown)

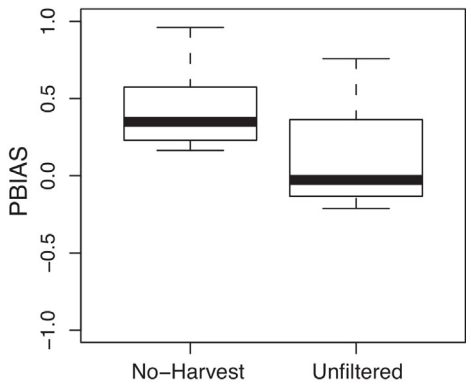

Fig. 6. Box plots of the PBIAS mismatch index (Equation 1) for community-level aboveground biomass (AGB). PBIAS was calculated for each forest type in each data set (No-Harvest or Unfiltered). Within each forest type, PBIAS reflects the difference between simulated and observed AGB across stand age classes (Fig. 5). Thick bars show medians, boxes show interquartile ranges, and whiskers show the minimum and maximum values.

suggested that these effects were weak, and apparently they are not needed to accurately predict species-level canopy layer statistics. In contrast, the better fit between predicted and observed PCAN for common species than for rare species (Fig. 4 and Fig. S1) suggests that sampling errors in FIA data contributed to PCAN errors. Accounting for this source of uncertainty should further reduce the discrepancies between predicted and observed PCAN.

4.2. Temporal and spatial heterogeneity in forest dynamics

Our results show how temporal non-stationarity in forest dynamics can cause model-data mismatches, because species whose abundances have increased over recent decades tended to have greater predicted than observed abundance. This is expected from non-stationarity if model parameters (e.g., growth and mortality rates) are estimated from recent inventory data and thus reflect recent competitive abilities, as in our study. Many factors may contribute to shifts in the competitive balance among species, including climate change and shifts in natural and/or human disturbance regimes (Condit et al., 1996; Franklin et al., 2005; Purves et al., 2008; Larocque et al., 2011). Identifying the factors leading to non-stationarity in different eastern U.S. forest types would be very useful, but also very data demanding, as it would require multi-decadal time series of both species demographic rates and environmental variables.

Our results also show that habitat specialization combined with edaphic variation within broad soil types has significant effects on forest community composition, because species tend to have more competitive parameter values in inventory plots where they are most abundant. This is consistent with previous studies documenting strong effects of edaphic heterogeneity on forest dynamics (e.g., Kobe, 1996; van Breemen et al., 1997), but is inconsistent with the alternative hypothesis that spatial variation in species composition is due primarily to dispersal limitation and stand history (McCune and Allen, 1985; Hubbell et al., 1999; Hubbell, 2001). The forest types defined in our study were based on ecoprovinces and coarse soil types reported by FIA (Fig. 1). Within each of our forest types, climate, soil, and other factors may be highly variable. In some cases, the causes of this variation may be apparent and relatively easy to account for (e.g., elevation and topographic position in mountainous regions), but species competitive abilities may also shift across a landscape due to less obvious forms of edaphic variation (e.g., Kobe, 1996). A potential solution is to use a finer soil type classification than the coarse one we adopted (xeric, mesic, or hydric soil), but this may be difficult due to the limited number of inventory plots in each soil type. Another option would be to estimate how growth and mortality rates vary as continuous functions of quantitative soil variables, such as those available from the U.S. Department of Agriculture Soil Survey Geographic (SSURGO) Database (http://soildatamart.nrcs.usda.gov/), although errors in soil data complicate this approach (Lichstein et al., 2014).

4.3. Additional factors contributing to model-data mismatches

The above results suggest that temporal and spatial heterogeneity contributed to mismatches between predicted dynamics and chronosequence observations, whereas canopy layer predictions from the simple flat-top PPA model were not an important source of error in our forest dynamics simulations. There are multiple

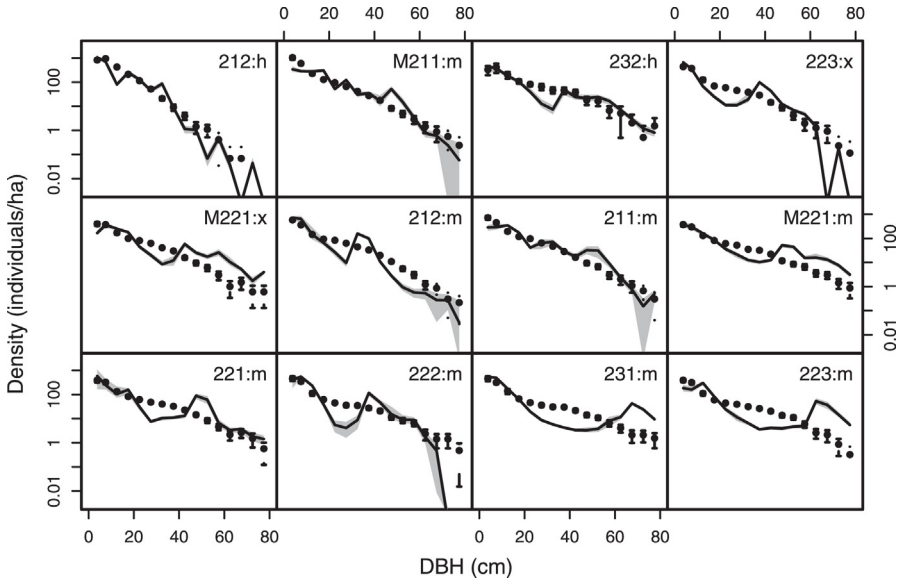

Fig. 7. Tree size distributions in mature forest in PPA simulations (95 year-old forest) and FIA data (90–100 year-old plots). Curves show the mean size distribution from 100 PPA simulations in each forest type (codes in the top right of each panel), and gray shading spans their 25th and 75th percentiles. See Fig. 4 for explanation of forest type codes and Fig. 5 for simulation methods. Points and error bars show FIA means and their 95% confidence intervals in 5-cm DBH classes. Results are for the No-Harvest case. Results for the Unfiltered case are in Fig. S2.

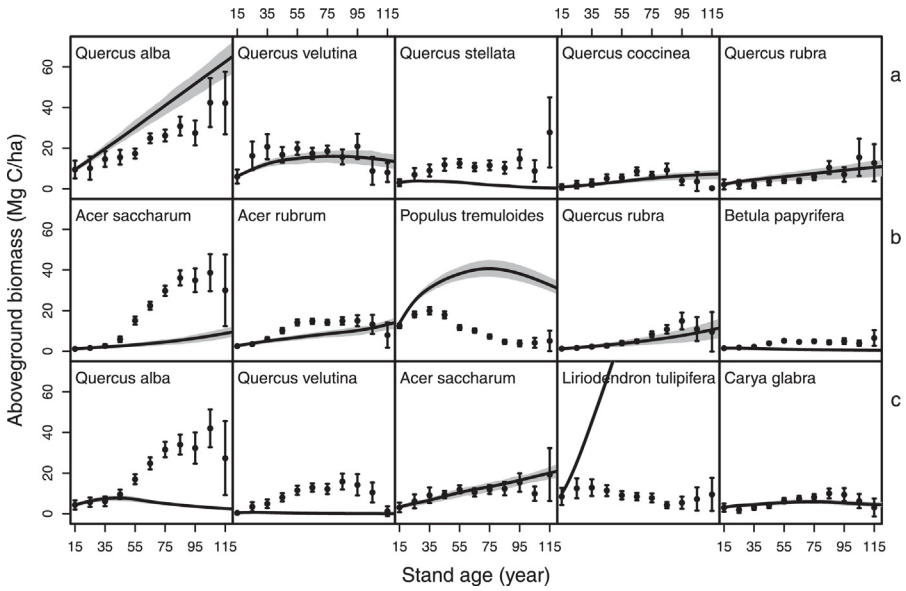

Fig. 8. Species-level aboveground biomass (AGB) dynamics in PPA simulations and FIA chronosequences for three selected forest types for the No-Harvest case (see Fig. 5a for community-level AGB). Within each forest type (row), the five most common species in the FIA data are arranged from left to right in order of decreasing abundance. (a) Forest type 223:x has a good PPA-FIA match at both community and species levels. (b) Forest type 212:m has a good community-level match but a poor species-level match. (c) Forest type 223:m has a poor match at both community and species levels. See Fig. 4 for explanation of forest type code and Fig. 5 for explanation of symbols and simulation methods.

additional factors that could complicate comparisons between predictions from forest dynamics models and chronosequences derived from forest inventory data. We now discuss some of the most likely sources of error in our model predictions and in forest chronosequences.

Firstly, errors in parameters describing demographic rates and allometry may cause model predictions to deviate from reality. For example, interspecific differences in fecundity, which we ignored, may contribute to model-data mismatches. Sampling errors for rare species may also result in large AGB mismatches if their growth and/or mortality rates contain large errors. These large errors may result in "super species" in models, with unrealistically high growth and/or survival rates. The probability that sampling errors will generate an apparent super species should increase with the number of species included in model simulations. We tested for this effect by sequentially eliminating the rarest species from our simulations, and then re-running the models with a reduced species set (results not reported). These experiments revealed no correlation between species number and the degree of model-data AGB mismatch, which suggests that super species (due to sampling errors) are not an important source of error in our simulations. This does not rule out the possibility that sampling errors, via some other mechanism, may have contributed to model-data mismatches.

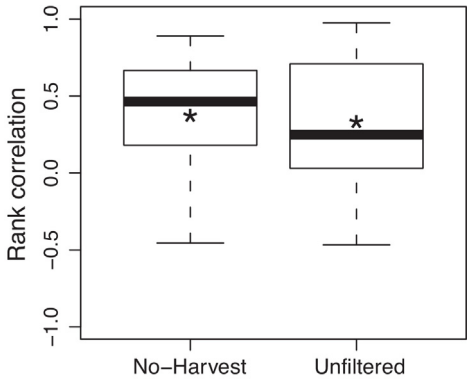

Fig. 9. Box plots of rank correlations between the species-level aboveground biomass mismatch index PBIAS (Eq. (1)) and the temporal trend in species abundance (ratio of post-1999 to pre-1999 species relative abundance in 20–40 year-old FIA plots) within forest types. One correlation was calculated across species within each forest type (12 No-Harvest forest types; 16 Unfiltered forest types). See Fig. 6 for explanation of box-plot symbols. Asterisks show rank correlations for all forest types combined (P-values = 5.1×10^{-5} and 1.2×10^{-4} for the No-Harvest and Unfiltered cases, respectively). The fraction of within-forest-type correlations that are positive is significantly different from the expected fraction under the null hypothesis that positive and negative correlations are equally likely (P-values = 0.003 and 0.006 for the No-Harvest and Unfiltered cases, respectively).

Secondly, incomplete information about stand disturbance history may affect our predictions. For example, although no harvesting was reported in the No-Harvest plots during their remeasurement intervals, some of these plots have likely been previously affected by selective logging, which is likely to influence long-term stand development. In contrast, for the Unfiltered case where selectively logged plots were included in mortality rate estimation, there was good agreement between community-level AGB predictions and chronosequence observations. Also, depending on the number of trees that survive a disturbance, the stand age reported by FIA (mean age of trees in dominant size class; Woudenberg et al., 2010) could be either the mean age of the surviving trees or an age much closer to zero. The uncertainty in the reported stand ages and/or problems with the stand-age concept in uneven-aged forests may introduce noise or systematic errors into FIA chronosequences.

Thirdly, our assumption of size-independent diameter-growth and mortality within each canopy layer may be overly simplistic. For large trees, mortality rates often increase (Lines et al., 2010; Dietze and Moorcroft, 2011) and diameter growth rates often decrease (Phipps, 1967; Martínez-Ramos and Alvarez-Buylla, 1998; Martínez Pastur et al., 2007) as diameter increases (depending on allometry, decreasing diameter growth rates are not necessarily inconsistent with increasing biomass growth rates; e.g., Stephenson et al., 2014). As noted in Section 2.2, including these effects in our model resulted in lower late-successional AGB predictions than those reported in Fig. 5, but had little impact on predicted species relative abundances. Thus while the assumption

Table 1
Evaluating the effects of spatial heterogeneity on model-data comparisons. θ_{ALL} refers to parameters estimated from the complete set (ALL) of FIA plots in a given forest type. θ_{HA} refers to parameters estimated from the dominant species' high-abundance (HA) plots in a given forest type. Tests were performed for all forest types in which parameter estimates were available for at least two species in both the ALL and HA cases.

	Initial condition[a]	Age class	Dominant match test (θ_{HA} vs. θ_{ALL})[b]	Dominant abundance test (HA > ALL)[c]
No-Harvest	Age 15, ALL	40–60	No (3/5 vs. 3/5)	5/5
	Age 15, HA	40–60	Yes (5/5 vs. 4/5)	5/5
	Age 0, none	40–60	Yes (2/5 vs. 1/5)	5/5
	Age 15, ALL	80–100	Yes (4/6 vs. 3/6)	6/6
	Age 15, HA	80–100	Yes (5/5 vs. 4/5)	5/5
	Age 0, none	80–100	No (5/6 vs. 5/6)	6/6
Unfiltered	Age 15, ALL	40–60	Yes (6/8 vs. 5/8)	8/8
	Age 15, HA	40–60	Yes (8/8 vs. 7/8)	8/8
	Age 0, none	40–60	Yes (3/8 vs. 2/8)	8/8
	Age 15, ALL	80–100	Yes (7/9 vs. 5/9)	9/9
	Age 15, HA	80–100	Yes (8/8 vs. 7/8)	8/8
	Age 0, none	80–100	Yes (8/9 vs. 6/9)	9/9

[a] Three initial conditions are: 15-year-old stands with initial cohorts from 10–20 year-old ALL plots (Age 15, ALL), 15-year-old stands with initial cohorts from 10–20 year-old HA plots (Age 15, HA), and 0-year-old stands with no initial cohorts (Age 0, none).
[b] "Yes" or "No" indicates whether or not the PPA model can better predict the most abundant species using θ_{HA} rather than θ_{ALL}. The numerator is the number of forest types in which simulations correctly predict the most abundant species. The denominator is the number of forest types tested.
[c] The numerator is the number of forest types in which θ_{HA} yielded higher predicted abundance of the dominant species than θ_{ALL}. The denominator is the number of forest types tested.

of size-independent diameter-growth and mortality may have introduced model errors, any such errors appear unrelated to species-level model-data mismatches. Alternatively, the assumption of size-independent diameter growth may be approximately correct over recent decades in the eastern U.S. due to growth enhancement associated with global change (e.g., nitrogen and/or CO_2 fertilization; Johnson and Abrams, 2009). In this case, recent growth enhancement (which was not accounted for by our model) would have contributed to mismatches between PPA-predicted dynamics and observed chronosequences.

4.4. Implications for testing broad-scale models of forest dynamics

Given the complications that spatial and temporal heterogeneity introduce into species-level model-data comparisons, a more practical approach to testing and developing forest dynamics models at broad geographic scales might be to adopt a functional-type-based approach (e.g., Vanderwel et al., 2013), as has been adopted in most dynamic global vegetation models (DGVMs; e.g., Foley et al., 1996; Sitch et al., 2003; Krinner et al., 2005). However, even in this case, we may expect complications due to spatial and temporal heterogeneity. For example, without the detailed information needed to account for heterogeneity, it may be unreasonable to expect to accurately predict the dynamics of functional types that co-occur within the same landscape (e.g., deciduous broad-leaved trees vs. conifers). In light of these complications, it may be useful to perform isolated tests of model structure that are not confounded with problems arising from spatial and temporal heterogeneity. Model structure may be assessed by comparing, for a given set of parameter values, predictions from simplified models such as the PPA to more complex models that are considered to be structurally correct. For example, Strigul et al. (2008) showed, for a two species-system, that the PPA model yields very similar predictions to a spatially-explicit individual-based forest simulator with phototropic branch growth. A more thorough evaluation of this nature may be useful for assessing the suitability of simplified forest dynamics models for adoption in next-generation DGVMs (Scheiter et al., 2013) that seek to represent individual-level competitive interactions. Along with model-data comparisons that span multiple temporal and spatial scales (e.g., Randerson et al., 2009), model-model comparisons designed to evaluate the consequences of simplifying assumptions in forest dynamics models may be a useful step in developing next-generation DGVMs.

Acknowledgements

We thank Mark Vanderwel, Trevor Caughlin, and two anonymous reviewers for valuable comments on an earlier draft. We thank Stephen Pacala and Drew Purves for useful discussions. Funding was provided by the USDA Forest Service Northern Research Station (Agreement 11-JV-11242306-059).

Appendix A. Supplementary methods and results

Supplementary methods and results associated with this article can be found, in the online version, at http://dx.doi.org/10.1016/j.ecolmodel.2014.02.011.

References

Adams, T.P., Purves, D.W., Pacala, S.W., 2007. Understanding height-structured competition in forests: is there an R^* for light? Proc. Biol. Sci. 274, 3039–3048.
Allen, C.D., Breshears, D.D., 1998. Drought-induced shift of a forest–woodland ecotone: rapid landscape response to climate variation. Proc. Natl. Acad. Sci. 95, 14839–14842.
Bechtold, W.A., Scott, C.T., 2005. The forest inventory and analysis plot design. In: Bechtold, W.A., Patterson, P.L. (Eds.), The enhanced Forest Inventory and Analysis program – national sampling design and estimation procedures. Gen Tech Rep: SRS-80. U.S. Department of Agriculture, Forest Service, Southern Research Station, pp. 27–42.
Bohlman, S., Pacala, S., 2012. A forest structure model that determines crown layers and partitions growth and mortality rates for landscape-scale applications of tropical forests. J. Ecol. 100, 508–518.
Canham, C.D., LePage, P.T., Coates, K.D., 2004. A neighborhood analysis of canopy tree competition: effects of shading versus crowding. Can. J. For. Res. 34, 778–787.
Caspersen, J.P., Vanderwel, M.C., Cole, W.G., Purves, D.W., 2011. How stand productivity results from size- and competition-dependent growth and mortality. PLoS ONE 6, e28660, http://dx.doi.org/10.1371/journal.pone.0028660.
Chesson, P., 2000. Mechanisms of maintenance of species diversity. Annu. Rev. Ecol. Syst. 31, 343–366.
Clark, J.S., Bell, D., Chu, C., Courbaud, B., Dietze, M., Hersh, M., et al., 2010. High-dimensional coexistence based on individual variation: a synthesis of evidence. Ecol. Monogr. 80, 569–608.
Condit, R., Hubbell, S.P., Foster, R.B., 1996. Changes in tree species abundance in a Neotropical forest: impact of climate change. J. Trop. Ecol. 12, 231–256.
Dietze, M.C., Moorcroft, P.R., 2011. Tree mortality in the eastern and central United States: patterns and drivers. Global Change Biol. 17, 3312–3326.
Dybzinski, R., Farrior, C., Wolf, A., Reich, P.B., Pacala, S.W., 2011. Evolutionarily stable strategy carbon allocation to foliage, wood, and fine roots in trees competing for light and nitrogen: an analytically tractable, individual-based model and quantitative comparisons to data. Am. Nat. 177, 153–166.
Farrior, C.E., Dybzinski, R., Levin, S.A., Pacala, S.W., 2013. Competition for water and light in closed-canopy forests: a tractable model of carbon allocation with implications for carbon sinks. Am. Nat. 181, 314–330.

Foley, J.A., Prentice, I.C., Ramankutty, N., Levis, S., Pollard, D., Sitch, S., et al., 1996. An integrated biosphere model of land surface processes, terrestrial carbon balance, and vegetation dynamics. Global Biogeochem. Cycles 10, 603–628.
Franklin, J., Syphard, A.D., He, H.S., Mladenoff, D.J., 2005. Altered fire regimes affect landscape patterns of plant succession in the foothills and mountains of southern California. Ecosystems 8, 885–898.
Friend, A.D., Stevens, A.K., Knox, R.G., Cannell, M.G.R., 1997. A process-based, terrestrial biosphere model of ecosystem dynamics (Hybrid v3.0). Ecol. Modell. 95, 249–287.
Hubbell, S.P., 2001. The Unified Neutral Theory of Biodiversity and Biogeography. Princeton University Press, Princeton, NJ, 448 pp.
Hubbell, S.P., Foster, R.B., O'Brien, S.T., Harms, K.E., Condit, R., Wechsler, B., et al., 1999. Light-gap disturbances, recruitment limitation, and tree diversity in a neotropical forest. Science 283, 554–557.
Jenkins, J.C., Chojnacky, D.C., Heath, L.S., Birdsey, R.A., 2003. National-scale biomass estimators for United States tree species. For. Sci. 49, 12–35.
Johnson, S.E., Abrams, M.D., 2009. Age class, longevity and growth rate relationships: protracted growth increases in old trees in the eastern United States. Tree Physiol. 29, 1317–1328.
Kardol, P., Todd, D.E., Hanson, P.J., Mulholland, P.J., 2010. Long-term successional forest dynamics: species and community responses to climatic variability. J. Veg. Sci. 21, 627–642.
Kobe, R.K., 1996. Intraspecific variation in sapling mortality and growth predicts geographic variation in forest composition. Ecol. Monogr. 66, 181–201.
Krinner, G., Viovy, N., de Noblet-Ducoudré, N., Ogée, J., Polcher, J., Friedlingstein, P., et al., 2005. A dynamic global vegetation model for studies of the coupled atmosphere–biosphere system. Global Biogeochem. Cycles 19, GB1015, http://dx.doi.org/10.1029/2003GB002199.
Larocque, G.R., Archambault, L., Delisle, C., 2011. Development of the gap model ZELIG-CFS to predict the dynamics of North American mixed forest types with complex structures. Ecol. Modell. 222, 2570–2583.
Lichstein, J.W., Dushoff, J., Ogle, K., Chen, A., Purves, D.W., Caspersen, J.P., et al., 2010. Unlocking the forest inventory data: relating individual tree performance to unmeasured environmental factors. Ecol. Appl. 20, 684–699.
Lichstein, J.W., Golaz, N.-Z., Malyshev, S., Shevliakova, E., Zhang, T., Sheffield, J., et al., 2014. Confronting terrestrial biosphere models with forest inventory data. Ecol. Appl., http://dx.doi.org/10.1890/13-0600.1 (in press).
Lichstein, J.W., Pacala, S.W., 2011. Local diversity in heterogeneous landscapes: quantitative assessment with a height-structured forest metacommunity model. Theor. Ecol. 4, 269–281.
Lichstein, J.W., Wirth, C., Horn, H.S., Pacala, S.W., 2009. Biomass chronosequences of United States forests: implications for carbon storage and forest management. In: Wirth, C., Gleixner, G., Heimann, M. (Eds.), Old-Growth Forests: Function, Fate and Value. Springer-Verlag, Berlin, Heidelberg, Germany, pp. 301–341.
Lines, E.R., Coomes, D.A., Purves, D.W., 2010. Influences of forest structure, climate and species composition on tree mortality across the eastern US. PLoS ONE 5, e13212, http://dx.doi.org/10.1371/journal.pone.0013212.
Martínez Pastur, G., Lencinas, M.V., Cellini, J.M., Mundo, I., 2007. Diameter growth: can live trees decrease? Forestry 80, 83–88.
Martínez-Ramos, M., Alvarez-Buylla, E.R., 1998. How old are tropical rain forest trees? Trends Plant Sci. 3, 400–405.
McCune, B., Allen, T.F.H., 1985. Will similar forests develop on similar sites? Can. J. Bot. 63, 367–376.
McNab, W.H., Cleland, D.T., Freeouf, J.A., Keys, Jr., J.E., Nowacki, G.J., Carpenter, C.A., (Comps.), 2007. Description of ecological subregions: sections of the conterminous United States. Gen Tech Rep: WO-76B. U.S. Department of Agriculture, Forest Service 80 pp.
Moorcroft, P.R., Hurtt, G.C., Pacala, S.W., 2001. A method for scaling vegetation dynamics: the Ecosystem Demography Model (ED). Ecol. Monogr. 71, 557–586.
Orwig, D.A., Cogbill, C.V., Foster, D.R., O'Keefe, J.F., 2001. Variations in old-growth structure and definitions: forest dynamics on Wachusett Mountain, Massachusetts. Ecol. Appl. 11, 437–452.
Pacala, S.W., Canham, C.D., Saponara, J., Silander Jr., J.A., Kobe, R.K., Ribbens, E., 1996. Forest models defined by field measurements: estimation, error analysis and dynamics. Ecol. Monogr. 66, 1–43.
Pacala, S.W., Canham, C.D., Silander Jr., J.A., Kobe, R.K., 1994. Sapling growth as a function of resources in a north temperate forest. Can. J. For Res. 24, 2172–2183.
Phipps, R.L., 1967. Annual growth of suppressed chestnut oak and red maple: a basis for hydrologic inference. Professional Paper: 485-C. U.S. Geological Survey, 27 pp.
Pickett, S.T.A., 1989. Space-for-time substitution as an alternative to long-term studies. In: Likens, G.E. (Ed.), Long-term Studies in Ecology: Approaches and Alternatives. Springer-Verlag, New York, pp. 110–135.
Purves, D.W., Lichstein, J.W., Pacala, S.W., 2007. Crown plasticity and competition for canopy space: a new spatially implicit model parameterized for 250 North American tree species. PLoS ONE 2, e870, http://dx.doi.org/10.1371/journal.pone.0000870.
Purves, D.W., Lichstein, J.W., Strigul, N., Pacala, S.W., 2008. Predicting and understanding forest dynamics using a simple tractable model. Proc. Natl. Acad. Sci. 105, 17018–17022.
Randerson, J.T., Hoffman, F.M., Thornton, P.E., Mahowald, N.M., Lindsay, K., Lee, Y.-H., et al., 2009. Systematic assessment of terrestrial biogeochemistry in coupled climate–carbon models. Global Change Biol. 15, 2462–2484.
Reams, G.A., Smith, W.D., Hansen, M.H., Bechtold, W.A., Roesch, F.A., Moisen, G.G., 2005. The Forest Inventory and Analysis sampling frame. In: Bechtold, W.A., Patterson, P.L. (Eds.), The enhanced Forest Inventory and Analysis program – national sampling design and estimation procedures. Gen Tech Rep: SRS-80. U.S. Department of Agriculture, Forest Service, Southern Research Station, pp. 11–26.
Sato, H., Itoh, A., Kohyama, T., 2007. SEIB–DGVM: a new Dynamic Global Vegetation Model using a spatially explicit individual-based approach. Ecol. Modell. 200, 279–307.
Scheiter, S., Langan, L., Higgins, S.I., 2013. Next-generation dynamic global vegetation models: learning from community ecology. New Phytol. 198, 957–969.
Sitch, S., Smith, B., Prentice, I.C., Arneth, A., Bondeau, A., Cramer, W., et al., 2003. Evaluation of ecosystem dynamics, plant geography and terrestrial carbon cycling in the LPJ dynamic global vegetation model. Global Change Biol. 9, 161–185.
Stephenson, N.L., Das, A.J., Condit, R., Russo, S.E., Baker, P.J., Beckman, N.G., et al., 2014. Rate of tree carbon accumulation increases continuously with tree size. Nature, http://dx.doi.org/10.1038/nature12914.
Strigul, N., Pristinski, D., Purves, D., Dushoff, J., Pacala, S., 2008. Scaling from trees to forests: tractable macroscopic equations for forest dynamics. Ecol. Monogr. 78, 523–545.
van Breemen, N., Finzi, A.C., Canham, C.D., 1997. Canopy tree–soil interactions within temperate forests: effects of soil elemental composition and texture on species distributions. Can. J. For. Res. 27, 1110–1116.
Vanderwel, M.C., Lyutsarev, V.S., Purves, D.W., 2013. Climate-related variation in mortality and recruitment determine regional forest-type distributions. Global Ecol. Biogeogr. 22, 1192–1203.
Walker, L.R., Wardle, D.A., Bardgett, R.D., Clarkson, B.D., 2010. The use of chronosequences in studies of ecological succession and soil development. J. Ecol. 98, 725–736.
Woudenberg, S.W., Conkling, B.L., O'Connell, B.M., LaPoint, E.B., Turner, J.A., Waddell, K.L., 2010. The Forest Inventory and Analysis Database: Database description and users manual version 4.0 for Phase 2. Gen Tech Rep: RMRS-GTR-245. U.S. Department of Agriculture, Forest Service, Rocky Mountain Research Station, Fort Collins, CO, 336 pp.
Yapo, P.O., Gupta, H.V., Sorooshian, S., 1996. Automatic calibration of conceptual rainfall-runoff models: sensitivity to calibration data. J. Hydrol. 181, 23–48.